

# Pocket Monte Carlo algorithm for classical doped dimer models

Werner Krauth<sup>1</sup> and R. Moessner<sup>2\*</sup>

<sup>1</sup>*CNRS-Laboratoire de Physique Statistique de l'Ecole Normale Supérieure*

<sup>2</sup>*Laboratoire de Physique Théorique de l'Ecole Normale Supérieure, CNRS-UMR8541  
24, rue Lhomond, 75231 Paris Cedex 05, France*

We study the correlations of classical hardcore dimer models doped with monomers by Monte Carlo simulation. We introduce an efficient cluster algorithm, which is applicable in any dimension, for different lattices and arbitrary doping. We use this algorithm for the dimer model on the square lattice, where a finite density of monomers destroys the critical confinement of the two-monomer problem. The monomers form a two-component plasma located in its high-temperature phase, with the Coulomb interaction screened at finite densities. On the triangular lattice, a single pair of monomers is not confined. The monomer correlations are extremely short-ranged and hardly change with doping.

## I. INTRODUCTION

Models of classical dimers on a lattice play an important role in polymer physics, but their statistical mechanics has proven to be of great value in a much wider range of settings. Prominently, in the early days of the resonating valence bond theories<sup>1</sup> of high-temperature superconductivity, Rokhsar and Kivelson<sup>2</sup> proposed that dimers could act as caricatures of singlet ('valence') bonds between spins  $1/2$ , with the hardcore condition on the dimer configurations translating the constraint that each spin participate in exactly one singlet bond with a neighboring spin. Resonances between different configurations generate a quantum dynamics for the resulting Rokhsar Kivelson quantum dimer models (RK-QDM).

These RK-QDMs are also of interest as effective theories, as they appear as limiting cases of  $d = 2 + 1$  dimensional Ising gauge theories which are dual to frustrated Ising models.<sup>3</sup> Central in this context is the question of confinement – can two test charges be separated infinitely far at finite cost in free energy? In the dimer model, these test charges are monomers, representing spinons or holons in the RVB theory.

In the context of RK quantum dimer models, *classical* dimer models play a crucial role because, for a particular choice of parameters, the quantum wavefunction is an equal-amplitude superposition of all classical dimer configurations.<sup>4</sup> For this reason, dimer-diagonal correlation functions can be obtained from the classical (equally weighted) average over all dimer configurations. At zero doping, such correlations can be obtained analytically using Pfaffian methods introduced by Kasteleyn<sup>5</sup> and developed further by a number of authors.<sup>6</sup> These methods have been extended to obtain correlation functions of a pair of monomers on the square lattice,<sup>7,8</sup> although it is not clear whether asymptotic monomer correlations can in general be obtained in closed form along those lines. Present analytical approaches do not allow an exact treatment of finite monomer densities; this is related to the absence of an analytical solution of the two-dimensional Ising model in a magnetic field.<sup>9</sup>

To reach the RK point in the presence of doping, it

is necessary not only to fine-tune two ratios of magnitudes of kinetic and potential energies but also a hopping phase.<sup>2</sup> This procedure is not innocuous, but classical correlations are also interesting because they are those of the quantum model at high temperature. There, hopping and resonance as well as any potential energies included in the dimer model are much smaller than the thermal energy. The classical correlations can remain non-trivial as a result of the projection onto the space of monomer-dimer coverings. One is thus interested in the presence of (at least short-range<sup>10</sup>) correlated structures, and how they change with doping.

In this paper, we present an efficient numerical algorithm for simulating classical monomer-dimer models. The algorithm is analyzed in some detail, and we mention possible uses for related problems.

Our main results are the following. Firstly, a pair of monomers on the triangular lattice is deconfined, with a correlation length of less than one lattice constant. This is in keeping with the very short-range *dimer* correlations on that lattice.<sup>11</sup> On the square lattice, the critical dimer correlations<sup>7</sup> generate a Coulomb interaction, with monomers on the same (different) sublattice having equal (opposite) charges. At finite density, the monomers form a two-dimensional two-component plasma in its Debye-screened high-temperature phase. For both square and triangular lattice, the monomer correlations decay monotonically with increasing density, without any sign of additional new correlations on any length scale.

We note that the study of monomer-dimer models goes back a long time.<sup>12</sup> However, we have not found in the literature an evaluation of the correlations studied here.

## II. POCKET ALGORITHM FOR MONTE CARLO SIMULATION OF DIMER MODELS

Overlaying two hardcore dimer configurations generates what is known as their transition graph; this graph consists of disjoint subgraphs of dimers alternating between the two configurations – such subgraphs are shown in Fig. 1.

An open graph, as shown on the left of Fig. 1, must

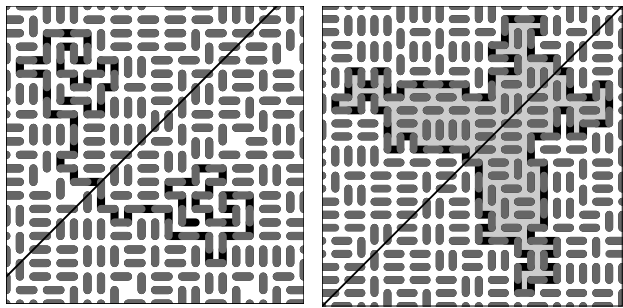


FIG. 1: Transition graphs of initial (black) and final (gray) configurations of the pocket algorithm presented in this paper. Left: In the presence of monomers the graph can be open; right: transition loop touching the symmetry axis. The cluster move consists in flipping the cluster - Note that we may also flip the dimers enclosed by a loop, and that the transition graph crosses the symmetry axis at most twice.

terminate on a monomer. Otherwise, it is a closed loop (a “transition graph loop”), as the one shown on the right of Fig. 1.

Any Monte Carlo move corresponds to a transition graph of the initial and final configurations. The simplest transition graphs arise from two pairs of dimers (for the square and triangular lattice) or from three (hexagonal lattice), which wind around a unit cell of the lattice. A Monte Carlo algorithm based on these local moves can have the same convergence problems as the local simulation methods for, e.g., the ferromagnetic Ising model near the Curie temperature due to critical slowing down. This problem is particularly acute for the square lattice dimer model, which has critical correlations. Elementary moves with many participating degrees of freedom can give rise to a substantial reduction of the Monte Carlo correlation time.

Several algorithms have been proposed to locate long connected transition graphs.<sup>14</sup> Typical problems in this context include diverging overhead (most of the time spent looking for a long loop is essentially wasted) and diminishing return (e.g. a long loop may end up invading the full system, or dynamically important moves may not be generated for sufficiently large systems). The ‘pocket algorithm’ we present here for hardcore dimers generates subgraphs from two configurations related by a global lattice symmetry. The algorithm obtains long transition graphs with minimal overhead: on lattices of size  $L \times L$ , no moves need to be rejected, and any dimer encountered during the construction participates in the move. In addition, there is no need for bookkeeping.

The pocket algorithm proceeds in a series of moves, at the beginning of which we randomly pick a symmetry axis, and a seed dimer (see Fig. 2). At this initial stage of the move construction, the seed is the sole element of a set  $\mathcal{P}$  (the ‘pocket’, filled with dark dimers), while all other (light gray) dimers belong to a set  $\mathcal{A}$ . Further in the move, dimers are shuffled around between sets  $\mathcal{A}$  and  $\mathcal{P}$  in the following way: At each step, an arbitrary

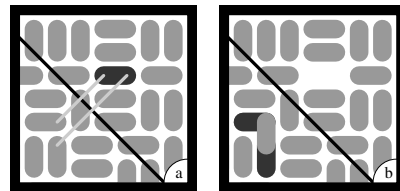


FIG. 2: Dimer algorithm. a: Symmetry axis and seed dimer (dark gray), sole initial element of the set  $\mathcal{P}$ , the ‘pocket’. b: An element of the pocket has been reflected with respect to the symmetry axis (and transferred from  $\mathcal{P}$  to  $\mathcal{A}$ , the set of regular dimers). It overlaps with two (dark) dimers, which are transferred from  $\mathcal{A}$  to  $\mathcal{P}$ . The move construction comes to an end when  $\mathcal{P}$  is empty.

element  $i$  of  $\mathcal{P}$  is reflected with respect to the symmetry axis, and moved to  $\mathcal{A}$ . If  $i$  overlaps with other elements of  $\mathcal{A}$  (dark dimers shown in Fig. 2b), the latter are moved from  $\mathcal{A}$  to  $\mathcal{P}$ . The move is completed as soon as the pocket  $\mathcal{P}$  is empty. During the whole construction, the algorithm keeps no memory of the graph, and final success is assured by the underlying symmetry of the lattice in combination with the hardcore property of the dimers.

The pocket algorithm is equivalent to the pivot-cluster algorithm,<sup>15</sup> which has been applied successfully to several hard-sphere problems.<sup>16,17</sup> It provides a greatly simplified implementation, as the Monte Carlo move is constructed without ever explicitly considering the cluster. In the specific application of dimer models, we also use reflections with respect to symmetry axes rather than point reflections. On the square lattice, for example, the algorithm is ergodic if we allow both diagonal and horizontal-vertical axes. The first choice allows to change the numbers of horizontal/vertical dimers, the second one permits to move through the different winding number sectors. The algorithm was tested against exact enumeration for systems up to size  $L = 6$ .

Transition graphs generated by the pocket algorithm, as shown in Fig. 1, are symmetric with respect to the symmetry axis, and cross it at most twice.

An analogous property holds in higher dimensions. For dimers on a three-dimensional lattice, for example, the appropriate operations are reflections with respect to randomly chosen symmetry planes of the (finite) lattice. Again, any transition graph is symmetric with respect to this symmetry plane, and crosses it at most twice. This places a strong constraint on the transition graph, which cannot invade space. If we used reflection with respect to a point, as was appropriate in other applications,<sup>15</sup> the move would conserve the total number of dimers of a given orientation, and also generate frequent transition graphs completely invading the lattice.

Transition loops generated by the algorithm allow to flip not only the loop itself but also all the dimers inside the (gray) loop area, which is symmetric with respect to the axis (see the example in Fig. 1). This modification, as well as simple generalizations where the pocket is initially populated by more than one dimer, or by a spe-

cially positioned dimer, have not yet been studied. We also note that this algorithm applies to other models that can be mapped onto (not necessarily nearest-neighbor) dimer models.<sup>18</sup>

For the undoped system on the square lattice, the pocket algorithm generates transition loops of average length proportional to  $L$ . A more detailed analysis is provided in the appendix.

### III. DIMER MODELS AT FINITE MONOMER DENSITY

We now turn to the problem of the correlations of monomers in a background of dimers on the square and triangular lattices. We evaluate the monomer two-point correlation function for a range of dopings.

The monomer two-point function is defined as follows. Let  $Z(r)$  be the partition function of the monomer-dimer problem with a monomer fixed at the origin and another at site  $r$ :  $Z(r)$  counts the number of allowed configurations subject to the pair of monomers being fixed. The two-point function is then defined to be proportional to  $Z(r)$ :  $C(r) \equiv Z(r)/Z_0$ ; the constant of proportionality,  $Z_0$ , is somewhat arbitrary. We choose to normalize the correlations such that a random distribution of monomers would give  $C(r) = 1$ . For the two-monomer problem however, to make contact with the previous literature,<sup>7</sup> we normalize the pair correlations such that (a)  $C(1) = 1/z$  and (b) list  $zC(r)$  in Tab. I, where  $z$  is the coordination of the lattice.

For the square lattice, the two-monomer correlations were obtained by Fisher and Stephenson<sup>7</sup> and by Hartwig<sup>8</sup> by perturbing the Pfaffian matrices introduced by Kasteleyn.<sup>5</sup> For the triangular lattice, there is as yet no analytic expression for the asymptotics of the monomer correlations,<sup>19</sup> and we have obtained the exact  $L = 6$  results by explicit enumeration.

#### A. The square lattice

To test the algorithm, first consider two-monomer correlations, calculated by several authors for the square lattice. In Fig. 3 and Tab. I, we compare our data against the analytical results. Note that the fit against the analytical asymptotic expression in Fig. 3 was done using a distance variable  $\tilde{r} = \sin(\pi r/L)/(\pi/L)$  to take into account periodic boundary conditions for a torus of length  $L$ .<sup>21</sup>

The fit is against the analytic asymptotic expression, and in Tab. I, we show a comparison of analytical and numerical results.<sup>20</sup> The results agree to within the numerical accuracy of  $10^{-3}$ , which improves even further for larger monomer densities,  $\rho$ , as the signal-to-noise ratio increases with the number of monomer pairs as  $\rho^2$ . A more accurate estimate could be obtained by finite-size scaling.

$r$	exact <sup>7</sup>	MC $L = 64$	exact $L = 6$	MC $L = 6$	MC $L = 12$
1	1	1	1	1	1
2	0.6366	0.638	0.8792	0.8789	0.8792
3	0.5947	0.595	0.8984	0.8980	0.8976
4	0.4821	0.484			0.8969
5	0.4506	0.452			0.8970
6	0.3995	0.402			0.8966

TABLE I: Monte Carlo versus exact results for monomer pair correlations,  $zC(r)$ , on the square (left) and triangular (right) lattices. The normalization here is  $zC(1) = 1$ . Even distances in the square lattice refer to sites on the adjacent row.<sup>7</sup> For the simulations presented here, the statistical error is about  $10^{-3}$  for both lattices.

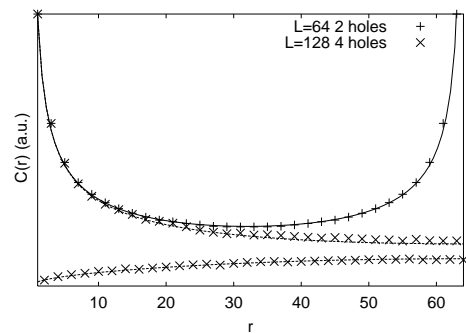


FIG. 3: Monomer correlations along a coordinate axis: (1) pair correlations on the square lattice with  $L = 64$ . The fit is to an analytic asymptotic expression generalized to include periodic boundary conditions. Same-sublattice correlations vanish. (2) Four monomers on a square lattice with  $L = 128$ . The lower curve corresponds to monomers on the same sublattice, the upper to monomers on different sublattices. The upper curve is again compared to the appropriate asymptotic function, whereas the lower curve is fitted to a power-law  $r^{1/2}$ . The deviation of the upper curve from the asymptotic expression for large  $r$  is due to screening.

For two monomers on opposite sublattices, the form of the correlations,  $C(r) = a_- r^{-1/2}$  defines an entropic Coulomb interaction between the two monomers:  $V(r) = -\frac{1}{2} \log r - \log a_-$ . Note that whereas the pair of monomers are critically confined –  $C(r) \rightarrow 0$  algebraically as  $r \rightarrow \infty$  – the expectation value of their separation grows with system size:  $\langle r \rangle \propto L$ .

As the square lattice is bipartite, dimers have one end on each sublattice. This means that on a torus, there are no dimer configurations with the two monomers present on the same sublattice: in this case,  $C(r) \equiv 0$ .

The question whether there is an effective interaction of the same form is nonetheless interesting. To avoid the sublattice constraint, we have investigated *four* monomers on a large lattice of size  $L = 128$ . For monomers on opposite sublattices, the results are essentially unaltered from the two monomer case, at least for separations which are not too large ( $r \ll L$ ); for

monomers on the same sublattice, we now obtain  $C(r) = a_+ r^{+1/2}$ , so that the monomers on each sublattice act as if they had equal and opposite Coulomb charge.

The  $L$ -dependence of the ratio  $a_-/a_+$  is fixed by the fact that the square lattice is at a critical point. This allows to write the finite-size scaling ansatz  $C(r) = \alpha L^{-2} c(r/L)$ , where  $c(x)$  is a function only depending on the ratio of  $r$  and  $L$ , and  $\alpha$  does not depend on  $L$ . The prefactor  $L^{-2}$  follows from the requirement that the area underneath the curves remain fixed as  $L \rightarrow \infty$ . With  $c_{\pm}(x) \propto x^{\pm 1/2}$ , we obtain  $a_-/a_+ \propto L$ . A fit for  $L = 128$  and four holes gives  $a_-/a_+ \approx L/2$ .

The dimers thus generate a Coulomb interaction for the monomers,  $V(r) = (qq'/2) \log r$ , with a sublattice-dependent sign of the monomer charge  $q$  ( $|q| = 1$ ). It is natural to expect this Coulomb interaction to be screened if the monomer density is finite, and their correlations to be no longer critical. In fact, for a finite density,  $\rho$ , of monomers, a new length scale arises, namely the average interparticle spacing,  $d \sim \rho^{-1/2}$ .

To analyze the details of the screening analytically, we model the monomer system by a classical, continuous two-dimensional two-component plasma. With a dimensionless coupling of  $\beta = 1/2$  (the prefactor of the logarithm), this plasma is located well in its high-temperature phase. This phase extends up to  $\beta = 2$ , where the continuum approximation breaks down as the plasma collapses in the absence of a repulsive hard core to the interaction.

In this high-temperature regime, we expect Debye screening to be operative. The resulting long-distance connected correlations have been obtained in Ref. 22 (where an expression going beyond Debye screening is given); they are

$$C(r) = 1 \pm \chi \sqrt{\frac{\pi \lambda_D}{2r}} \exp(-r/\lambda_D),$$

with the Debye screening length:  $\lambda_D = 1/\sqrt{2\pi\beta\rho}$ , and with  $\chi = \beta$  to lowest order in the coupling. The choice of sign depends on the sublattice.

With the new length scale,  $\lambda_D \propto d$ , the criticality of the correlations is destroyed, although the critical behavior remains visible for  $r \ll \lambda_D$ . This is why it was possible to find the two-particle interaction from the four-monomer problem above.

In order to determine whether this scenario is indeed realized for the monomer-dimer mixture, we have plotted  $C(r)$  versus the scaled distance  $r/\lambda_D$  for varying monomer densities for a system of size  $L = 64$  (Fig. 4).

From the form of the expression for  $C(r)$ , all curves should collapse on top of one another. However, for a finite system, one has to take into account the presence of two length scales,  $L$  and  $\lambda_D$ , with the added feature that  $\lambda_D < L$ , so that a simple one-parameter finite-size scaling ansatz no longer applies. For  $\lambda_D \ll L$  (large monomer densities), the collapse works indeed very well.

The data do not collapse at small densities, which is a finite-size effect: In Fig. 5, we plot the monomer correlations at a fixed monomer density  $\rho = 2/64^2$  for

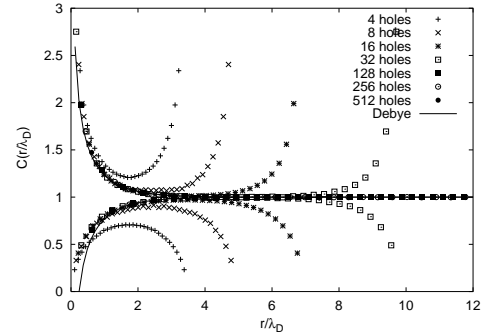


FIG. 4: Monomer correlations  $C$  for different monomer densities, against the scaled distance variable  $r/\lambda_D$ , for the square lattice with  $L = 64$ .

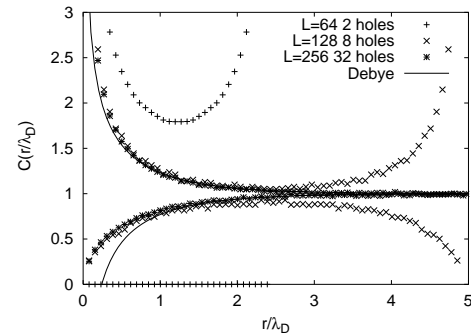


FIG. 5: Monomer correlations  $C$  against the scaled distance variable  $r/\lambda_D$  at fixed monomer density  $\rho = 2/64^2$  for square lattices of size  $L = 64, 128, 256$ .

$L = 64, 128$  and  $256$ . Whereas the two-hole problem suffers from the sublattice pathology, one can see that the data for  $L = 128$  and  $256$  collapse nicely for short distances, with disagreement arising for distances around  $L/2$  where the periodic boundary conditions become important.

In the region where they collapse, the curves in Figs. 4 and 5 agree with the asymptotic Debye prediction for large values of  $r/\lambda_D$ . At small  $r$ , the effectively unscreened behavior is visible, leading again to a unique curve for  $C(r)$ .

## B. The triangular lattice

Dimer correlations on the triangular lattice are known to be short-ranged,<sup>11</sup> and not critical as is the case for the square lattice.<sup>7</sup> This leads one to expect that the monomer correlations will also be short-ranged as the presence of a monomer should have little effect at a distance large compared to the dimer correlation length.

We have plotted the correlations of a pair of monomers in the inset to Fig. 6. The correlation length indeed is so small that already for a triangular lattice of size  $L = 12$ , finite-size effects are no longer detectable. This is also

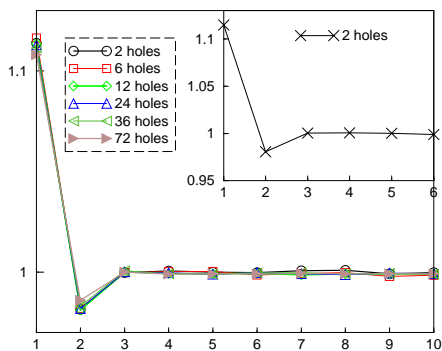


FIG. 6: Monomer correlations  $C_r$  along a coordinate axis at variable doping for a lattice of size  $L = 24$ . The abscissa is in units of lattice spacings. Correlations are normalized against a random distribution. Inset: two-monomer correlation in a lattice of size  $L = 12$ . In both cases, the  $x$ -axis denotes separation along one of the lattice vectors. Note that the  $y$ -axis only varies by less than 15%.

shown in Tab. I.

At ‘large’ distances, the correlations tend to a constant, nonzero value of  $C(\infty) = 0.1495 \pm 0.0001$ . (This value is given, in keeping with the convention of the square lattice case, with a normalization such that  $C(1) = 1/6$ .) They do so with an extremely short correlation length, which we cannot determine accurately as there are only about 3 data points above the noise level. This makes it hard to fit an asymptotic form, as the presence of a power-law and/or oscillatory multiplicative factor cannot be detected on this basis. From the absence of any signal for distances beyond  $r = 3$ , we conclude that the correlation length is less than one lattice spacing.

This nonzero large-distance limit of the monomer correlation function implies that monomers in the classical hardcore dimer model on the triangular lattice are deconfined – the free energy for monomers a distance  $r$  apart does not diverge as  $r \rightarrow \infty$ . This contrasts with the square lattice, where this quantity diverges logarithmically.

Upon further doping, the correlations barely change (see Fig. 6); a small decrease of the correlations only becomes visible for a doping level of  $1/8$ . This is not unexpected as the average monomer spacing always remains well above the two-monomer correlation length.

#### IV. CONCLUSION

We have studied the correlations of monomer-dimer mixtures on the square and triangular lattices with a new Monte Carlo algorithm. The monomers interact via the background of dimers: the critical correlations of the dimers on the square lattice give rise to a two-monomer interaction of long-range Coulomb nature, whereas the disordered triangular correlations generate an exponentially decaying one.

The triangular model is deep in its disordered phase,

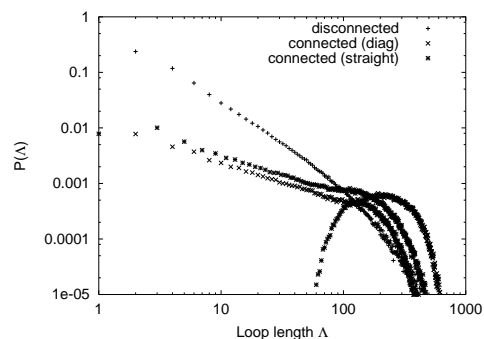


FIG. 7: Distribution of transition loop lengths for the square lattice with  $L = 64$ .

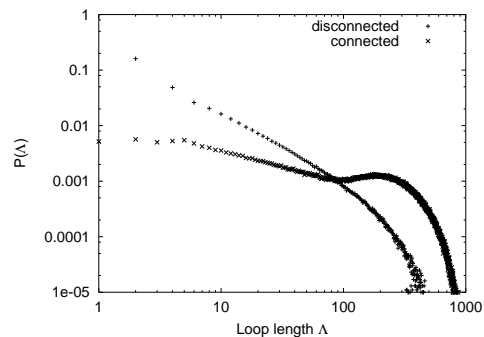


FIG. 8: Distribution of transition loop lengths for the triangular lattice with  $L = 64$ .

where it remains in the presence of a finite density of monomers. The square model, located at a phase boundary, is driven into a disordered phase on doping. This effect is rendered analytically by modeling the monomers as a two-dimensional two-component plasma, with the long-range correlations given by a simple Debye-screened form.

#### Appendix

In this appendix, we analyze the distribution of transition graph lengths in the undoped dimer model, where only loops are generated. These loops can be of several types: disconnected pairs of loops not touching the symmetry axis, connected loops passing through the symmetry axis, but not winding around the box, and finally those winding around the box. Each of these distributions strongly depends on the lattice and on the details of the choice of axes. The distribution of loop lengths,  $\Lambda$ , generated by the pocket algorithm is shown in Fig. 7 for the square lattice. Whereas the disconnected loops follow a nice power law distribution  $P(\Lambda)_{\text{disconnect}} \sim \Lambda^{-1.5}$  for  $\Lambda < L$ , and are always made up of an even number of dimers, the connected loops are distributed as  $P(\Lambda)_{\text{connect}} \sim \Lambda^{-0.75}$ . For the reflection about a diagonal, the loop lengths are always even, whereas they

are odd for the horizontal-vertical reflections that do not wind around the lattice. If a loop does wind around the box, its length can be odd or even. Notwithstanding this intricate structure, we find that the mean loop length grows as  $L^\mu$ , with  $\mu = 1.00 \pm 0.01$ . On the triangular lattice, the distribution of loop lengths is also nicely split into connected and disconnected loops (see Fig. 8). There, we find for the mean loop length  $\mu = 1.47 \pm 0.02$ . We note that the algorithm is biased towards longer subgraphs of the transition graph of a configuration with its reflection with a factor proportional to their length.

Finally, it would be interesting to analyze the expo-

nents in more detail, in particular as the square model maps onto a height model,<sup>23</sup> whereas the triangular one does not.<sup>24</sup>

### Acknowledgements

RM would like to thank John Chalker, Paul Fendley, David Huse, Jane Kondev and Shiyaji Sondhi for useful discussions.

- 
- \* Electronic address: krauth@lps.ens.fr; moessner@lpt.ens.fr
- <sup>1</sup> P. W. Anderson, *Science* **235**, 1196 (1987).
  - <sup>2</sup> D. S. Rokhsar and S. A. Kivelson, *Phys. Rev. Lett.* **61**, 2376 (1988).
  - <sup>3</sup> R. Moessner, S. L. Sondhi and E. Fradkin, *Phys. Rev. B* **65**, 024504 (2002)
  - <sup>4</sup> This is in fact only true for each *sector* separately – see e.g. Ref. 2.
  - <sup>5</sup> P. W. Kasteleyn, *Physica* **27**, 1209 (1961)
  - <sup>6</sup> For a review, see J. F. Nagle, C. S. O. Yokio and S. M. Bhattacharjee, “Dimer models on anisotropic lattices”, in *Phase Transitions and Critical Phenomena*, ed. by C. Domb and J. Lebowitz, v. 13 (Academic Press, 1980).
  - <sup>7</sup> M. E. Fisher and J. Stephenson, *Phys. Rev.* **132**, 1411 (1963).
  - <sup>8</sup> R. E. Hartwig, *J. Math. Phys.* **7**, 286 (1966)
  - <sup>9</sup> P. W. Kasteleyn, *J. Math. Phys.* **4**, 287 (1963).
  - <sup>10</sup> O. J. Heilmann and E. H. Lieb *Phys. Rev.* **24**, 1412 (1970). These authors showed that the free energy of non-interacting monomer-dimer mixtures can be non-analytical as a function of density and temperature only in the limit of vanishing density.
  - <sup>11</sup> R. Moessner and S. L. Sondhi, *Phys. Rev. Lett.* **86**, 1881 (2001).
  - <sup>12</sup> R. H. Fowler and G. S. Rushbrooke, *Trans. Faraday Soc* **33**, 1272 (1937).
  - <sup>13</sup> M. E. Fisher, *Phys. Rev.* **124**, 1664 (1961).
  - <sup>14</sup> G. T. Barkema and M. E. Newman, *Phys. Rev. E* **57**, 1155 (1998) and references therein.
  - <sup>15</sup> C. Dress and W. Krauth, *J. Phys. A* **28**, L597 (1995).
  - <sup>16</sup> A. Buhot and W. Krauth, *Phys. Rev. Lett.* **80**, 3787 (1998), *Phys. Rev. E* **59**, 2939 (1999).
  - <sup>17</sup> L. Santen and W. Krauth, *Nature* **405**, 550 (2000).
  - <sup>18</sup> M. E. Fisher, *J. Math. Phys.* **7**, 1776 (1966).
  - <sup>19</sup> Although an asymptotic form is missing, the monomer correlation function has been obtained recursively for finite distances in parallel with this work by P. Fendley, R. Moessner and S. L. Sondhi, *in preparation*.
  - <sup>20</sup> For these simulations, the initial seed of the pocket algorithm was chosen to be one of the monomers.
  - <sup>21</sup> By conformal invariance, this form is strictly applicable only for an infinite strip of width  $L$  for a system with critical correlations.
  - <sup>22</sup> L. Samaj and B. Jancovici, *J. Stat. Phys.* **106**, 301 (2002); *J. Stat. Phys.* **106**, 323 (2002).
  - <sup>23</sup> J. Kondev and C. L. Henley, *Phys. Rev. Lett.* **74**, 4580 (1995).
  - <sup>24</sup> R. Moessner, S. L. Sondhi and P. Chandra, *Phys. Rev. Lett.* **84**, 4457 (2000), R. Moessner and S. L. Sondhi, *Phys. Rev. B* **63**, 224401 (2001).